HHS Public Access

Author manuscript

Radiother Oncol. Author manuscript; available in PMC 2019 December 01.

Published in final edited form as:

Radiother Oncol. 2018 December ; 129(3): 589–594. doi:10.1016/j.radonc.2018.06.016.

UV scintillating particles as radiosensitizer enhance cell killing after X-ray excitation

Matthias Müller[a], **Yimin Wang**[b], **Michael R. Squillante**[b], **Kathryn D. Held**[c], **R. Rox Anderson**[a], and **Martin Purschke**[a,*]

[a]Wellman Center for Photomedicine, Massachusetts General Hospital/Harvard Medical School, Boston

[b]Radiation Monitoring Devices, Inc., Watertown

[c]Department of Radiation Oncology, Massachusetts General Hospital/Harvard Medical School, Boston, United States

Abstract

Background and purpose: Radiation therapy is the gold standard treatment for inoperable malignant tumors. However, due to the heterogeneity of the tumor, some regions are more radio resistant and can lead to metastasis and tumor recurrence. In this study, we propose combining traditional X-ray treatment with UVC-emitting $LuPO_4:Pr^{3+}$ nanoparticles (NPs) to increase the tumor control as well as to reduce tumor recurrence and metastasis. These NPs convert ionizing radiation into UVC-photons (UVC range: 200–280 nm) locally at the tumor site. Unlike X-ray, UVC-photons damage DNA directly via an oxygen-independent mechanism, which could improve treatment of radioresistant tumors such as hypoxic tumors.

Materials and methods: The effect of X-ray generated UVC-photons was tested on human fibroblasts incubated with NPs prior to radiation treatment. The surviving fraction of the cells was assessed by means of colony formation assay. Experiments were performed on normal and UVC sensitive cell lines to demonstrate the presence of UVC photons during treatment. In addition, UV-specific DNA damages were investigated using an immunofluorescence assay to measure cyclopyrimidine dimers (CPDs).

Results: Combined treatment showed an increased cell death of over 50%, compared to radiation alone. This results in a dose equivalent of 4 Gy for the combined treatment with 2 Gy irradiation. The formation of CPDs and the increased effect on UV sensitive cells indicate the presence of UV photons. The generated amount of CPDs is comparable to an UVC exposure of about 15 $J \times m^{-2}$.

Conclusion: Combining NPs with ionizing radiation results in a localized dose surge, which could increase tumor control. It could also allow lowering the total applied dose to minimize unwanted side effects to the surrounding normal tissue while maintaining tumor control.

*Corresponding author at: Wellman Center for Photomedicine, Their 201A, Massachusetts General Hospital/Harvard Medical School, 40 Blossom Street, Boston, MA 02114, United States.

Conflicts of interest

None.

Keywords

UV radiation; Cancer treatment; Radiation therapy; Radiosensitizer

Cancer is a major cause of mortality worldwide. In 2012, 14 million new cancer cases and 8 million deaths attributed to cancer occurred [1]. Currently, radiation therapy is the gold standard for many inoperable malignant tumors. Nearly 50% of patients with solid tumors undergo radiation therapy during the course of their disease [2]. Some tumors, in particular tumors with hypoxic areas, are generally more radiation resistant and are thought to be responsible for a poor outcome of the treatment, the formation of metastasis and tumor recurrence [3]. To overcome this radioresistance and to avoid unwanted side effects on normal tissue fractionated treatments with complex irradiation plans are used. Radiation therapy also causes dose-dependent deleterious side effects such as fibrosis in normal tissues which are traversed during the therapy [4,5].

Nanoparticles (NPs) as radiosensitizers combined with X-rays is a promising approach to increase tumor control. In particular, gold NPs have been studied to increase the local dose of ionizing radiation at the tumor site to enhance the absorption of energy in the tumor causing increased DNA damage [6,7]. Also, Hf, Bi, and rare earth elements such as Gd are of particular interest as radiosensitizers [8–10]. Due to their high atomic number z these elements provide a large absorption cross section for X-ray radiation, which leads to emission of lower energy radiation resulting in a higher local dose at the desired target. These high Z elements also produce more photoelectrons as well as Auger electrons, which generate reactive radicals to additionally damage the tumor cells. Nevertheless, the radiosensitizing effect of these elements is still O_2–dependent.

This study focuses on the hypothesis to generate ultraviolet (UV) radiation in proximity of cells to increase cell death. Unlike ionizing radiation, UVC radiation between 200 and 280 nm efficiently kills cells directly through oxygen-independent photochemistry [11]. We combine traditional X-ray treatment with an UV emitting radiosensitizer such as $LuPO_4$:Pr^{3+} to generate localized UVC photons. $LuPO_4$:Pr^{3+} converts X-rays into UVC radiation due to the inter-configurational $4f^1 5d^1$-$4f$ transition in Pr^{3+} resulting in an intense emission band in the spectral range of 220–285 nm [12]. In addition, $LuPO_4$:Pr^{3+} provides a high density and high z-number to ensure sufficient absorption of the X-ray radiation to increase local radiation dose as previously described for gold [13]. The conversion of high energy X-rays into low energy X-rays due to the high density of the undoped $LuPO_4$ host material was investigated and compared to the doped $LuPO_4$:Pr^{3+} in detail by Squillante et al. [14].

UV radiation produces two major types of DNA damage, cyclobutane pyrimidine dimers (CPDs) and 6–4 photoproducts (6-4PPs), that can lead to a permanent cell cycle arrest followed by cell inactivation. UVC photons are strongly absorbed within a few micrometers [15], so that cells in the immediate vicinity of the scintillating particles would be affected, while surrounding normal tissue would be spared from UVC exposure. Due to fenestrations in cancer blood vessels, intravenously injected nanoparticles preferentially deposit in solid tissue tumors [16]. This is called ehanced permeability and retention effect (EPR). Delivery

of UVC scintillating particles to cancerous tumors could potentially enhance the effectiveness of radiation therapy. Experiments were performed to test the hypothesis whether UVC scintillating nanoparticles can enhance cell lethality after exposure to X-ray radiation.

Materials and methods

Cell lines

Experiments were performed with a normal human foreskin fibroblast cell line (HFF1, ATCC® SCRC-1041™, Manassas, VA) and with a particularly UV-sensitive human fibroblast cell line (XP17BE, ATCC® CRL-1360™, Manassas, VA) obtained from xeroderma pigmentosum patient. Cells were cultured in Dulbecco's Modified Eagle Medium (DMEM) (Life Technologies, Carlsbad, CA) supplemented with 1% Pen/Strep solution (10000 U × ml^{-1} penicillin, 10000 μg × ml^{-1} streptomycin, Life Technologies, Carlsbad, CA) and 10% fetal bovine serum (Life Technologies, Carlsbad, CA). Cells were cultured at 37 °C in a humidified atmosphere of 95% air and 5% CO_2 and used for experiments in passage 3–12.

Dispersion of NPs

$LuPO_4:Pr^{3+}$ NPs were obtained from Radiation Monitoring Devices, Inc. (RMD, Watertown, MA). The size of the $LuPO_4:Pr^{3+}$ particles was about 50–200 nm (Fig. 1). $LuPO_4:Pr^{3+}$ dispersions with 0.5,1.0, 2.5, 5.0, and 7.5 mg × ml^{-1} were prepared by dispersing the $LuPO_4:Pr^{3+}$ powder in DMEM using 0.01% Darvan C (Vanderbilt Minerals, LLC, Norwalk, CT) as a dispersing agent. The dispersion was treated with ultrasound (Cole-Parmer 8852, Vernon Hills, IL) for 15 min and thoroughly mixed before used. 1.5 ml of the dispersion was applied onto cells. At the time of X-ray irradiation, the majority of the NPs were settled down in close proximity to the cells.

X-ray irradiator

Cells in 12.5 cm^2 cell culture flasks were irradiated with X-rays with a biological irradiator X-RAD 320 (Precision X-Ray, North Branford, CT) at a dose rate of 450 cGy × min^{-1}. Acceleration voltage and anode current were 320 kV and 12.5 mA, respectively. A 2-mm thick Al-filter was used to harden the X-ray beam.

Transmission electron microscopy

Particle size and morphology were investigated using transmission electron microscopy (TEM) (Philips CM10, Eindhoven). The TEM was equipped with a digital camera system (Advanced Microscopy Techniques, Woburn, MA) and a Tungsten anode. Samples were prepared by putting the powder on a Cu grid coated with SiO-treated Formvar (Ted Pella, Inc. Redding, CA). Residual powder was removed by tapping the grid. Images were recorded with acceleration voltage of 80 kV.

Spectroscopy

The emission spectrum of $LuPO_4:Pr^{3+}$ was recorded on an Edinburgh Instruments FSL900 spectrometer equipped with an X-ray excitation source (Neptune 5200, Oxford Instruments, Abigdon, GB). Acceleration voltage and anode current were 50 kV and 2 mA, respectively.

Colony formation assay

Clonogenic cell survival was assessed using the colony formation assay. 150,000 cells were seeded in 12.5 cm^2 tissue culture flasks (Falcon®, Corning, NY) 24 h before the experiment. Cells were incubated with NPs for 15 min before irradiation with 2 Gy × ray. Immediately after irradiation, cells were washed gently with DMEM to remove the NPs. Cells were harvested and replated afterwards in triplicate at 100 or 200 non-irradiated cells or 200 or 400 irradiated cells into six-well plates. After 14 days, cells were fixed using 1 ml of 10% phosphate buffered Formalin (per well. After 1 h, colonies were stained with crystal violet solution (0.001 mg × l^{-1}) for 24 h and counted.

Detection of cyclopyrimidine dimers

UV-specific DNA damages were detected by using the immunochemistry staining assay for CPDs (OxiSelect (CPD), Cell Biolabs, Inc. San Diego, CA). The analysis was performed according to the manufacturer's protocol. Briefly, cells were seeded to be 80–90% confluent in 96-well plates. After irradiation, cells were immediately washed, fixed and incubated with the monoclonal CPD-antibody followed by secondary horseradish peroxidase antibody. Quantification of the CPDs was performed with an ELISA plate reader (SpectraMax M5, Molecular Devices, LLC, San Jose, CA) by measuring the absorbance at 450 nm.

Statistical analysis

The software GraphPad Prism version 7.03 for Windows was used (GraphPad Software, La Jolla, CA). Data were presented as mean ± standard deviation. Statistical analysis was performed applying a Two-way ANOVA with Tukey's and Sidak's multiple comparisons tests. p values < 0.05 were considered statistically significant.

Results

Characterization of $LuPO_4:Pr^{3+}$ NPs

Size and morphology of the $LuPO_4:Pr^{3+}$ NPs were investigated by optical microscopy and TEM. The optical microscope image of HFF1 cells with NPs (bright dots) is shown in Fig. 1a. The picture suggests the particle size to be in the nanometer range. However, a few larger agglomerations of particles were noted. The TEM images confirm the size range of the NPs. Fig. 1b shows a TEM image of a cluster of the $LuPO_4:Pr^{3+}$ particles with particle sizes up to 200 nm. A single NP is depicted in Fig. 1c with an approximate size of 125 nm. Further, the NPs possess a smooth surface and almost spherical shape.

The emission spectrum of the $LuPO4:Pr^{3+}$ NPs is shown in Fig. 2. The spectrum was recorded under X-ray excitation and shows four intense emission bands in the UVC region, ranging from about 220–285 nm, as well as a few weaker bands in the visible range peaking around 600 nm. The emission peaks at 235, 245, 263, and 274 nm can be attributed to the

characteristic inter-configurational $4f^1 5d^1$-$4f^2$ transition in Pr^{3+}. The emission in the visible region of the spectrum is due to the intra-configurational $4f^2$-$4f^2$ transition.

Cytotoxicity and radiosensitization effect of $LuPO_4$:Pr^{3+} NPs

The HFF1 cell line showed a dose depending decrease in surviving fraction after X-ray treatment, which is in accordance to the literature (Fig. 3) [17,18]. Combined treatment with X-ray and $LuPO_4$:Pr^{3+} NPs resulted in increased cell inactivation (Fig. 4). The surviving fraction of the non-irradiated cells incubated with the lower concentrations (0.5, 1.0, and 2.5 mg × ml^{-1}) of $LuPO_4$:Pr^{3+} did not change significantly. On the other hand, higher concentrations of 5.0 and 7.5 mg × ml^{-1} $LuPO_4$:Pr^{3+} caused a significant concentration-dependent decrease in surviving fraction of about 25 and 35%, respectively. Radiation treatment with 2 Gy alone resulted in a decrease of the surviving fraction to about 30%. Combined treatment with increasing $LuPO_4$:Pr^{3+} concentration showed a concentration dependent decrease of the surviving fraction up to 2% for 7.5 mg × ml^{-1}.

Cytotoxicity of XP and normal fibroblast cell lines

To confirm a UVC specific effect, UVC sensitive fibroblast cell line (XP17BE) was compared to normal fibroblasts (HFF1). Fig. 5 illustrates the colony formation assay for both cell lines after irradiation with 2 Gy in the presence of 2.5 mg × ml^{-1} $LuPO_4$:Pr^{3+}. Both cell lines did not show significant differences in radiation sensitivity and unspecific toxicity of the NPs. The surviving fraction of normal fibroblasts decreased to 25%, whereas the surviving fraction of the UV sensitive cell line decreased to 15%.

UV specific DNA damage

UV specific DNA damage was detected using a commercially available immunochemistry assay for CPDs. The amount of CPDs generated after irradiation of the cells with an X-ray dose of 4 Gy in combination with NPs, as well as for radiation and NPs alone is shown in Fig. 6. UVC radiation with a wavelength of 254 nm and a dose of 60 J × m^{-2} was used as a positive control. Raw ELISA data are shown in Fig. 6a and normalized data are shown in Fig. 6b. For normalization, the amount of CPDs produced after UVC was set to 100% and the control was set to 0%. NPs and radiation alone revealed a non-significant increase of CPDs of about 10 and 15%, respectively. The combined treatment of irradiation and NPs generated a significant increase of CPDs of about 50%.

Discussion

Radiation therapy is a widely-used treatment for cancer, but has major limitations. To improve tumor control, radiosensitizing drugs as well as NPs have been studied in recent years [6,19]. This is the first study using UVC emitting NPs to enhance cell killing by X-rays. We observed that $LuPO_4$:Pr^{3+} particles with a broad emission maximum in the range of 220–285 nm significantly enhance cell lethality from X-ray irradiation. Furthermore, we found the mechanism of enhanced lethality to be consistent with UV-induced DNA damage, as evidenced by a significant increase in CPD photoproducts, and greater effect in XP cells that are specifically deficient in repairing UV-induced DNA damage. The potential therefore

exists, to use UVC scintillating particles delivered into tumors, to improve outcomes of radiation therapy.

Unlike ionizing radiation, UVC-induced cell killing is largely oxygen independent, but the oxygen dependence of X-ray injury enhanced by UV scintillating particles has yet to be studied. Oxygen is not directly involved in the formation of CPDs, the major DNA photoproduct of UVC associated with cell death. However, reactive oxygen species may play a substantial role in downstream response pathways [20]. UVC "germicidal" lamps are widely used for environmental air and water purification. Direct, non-oxygen-dependent damage to DNA occurs, but photochemical generation of ozone from atmospheric oxygen, and some oxygen-dependent photochemical reactions may also be involved. In our study, UVC radiation was not applied externally, but generated locally after X-ray excitation. The results strongly suggest that UVC emission from scintillating particles delivered within a solid tissue tumor would increase the efficiency of cell killing after X-ray exposure. We surmise that additional efficacy would be gained by the relative lack of oxygen-dependence for UVC cell killing, but this remains to be determined.

We used a primary particle size ranging from 50–200 nm (Fig. 1), which is much smaller than cells or cell nuclei. Insoluble particles in this size range are typically phagocytosed by cells in human tissues, which is the basis for skin tattoos, in which most of the "ink" is intracellular [21]. A large portion of scintillating NPs delivered into tissues including tumors are likely to become phagocytosed. However, previous studies with gold nanoparticles have found reduced cellular uptake in the hypoxic region of tumors [22]. In our study, most of the particles were not intracellular, as shown in Fig. 1a, due to the short incubation time of 15 min. The uptake of the particles will be investigated in future experiments. The $LuPO_4$: Pr^{3+} NPs used in this work were not stabilized or functionalized. Therefore, the larger particles we observed by electron and optical microscopy arise from agglomeration of the smaller particles in aqueous solution. It is not uncommon for NPs to form larger agglomerates, since this process decreases the surface area and its associated free energy. We observed that suspending the NPs in cell culture medium with serum reduced the agglomeration compared to suspending them in H_2O. Spontaneous alignment of proteins and/or natural surfactant molecules at the particle surfaces could limit agglomeration. Nonetheless, agglomerations still occur to a certain degree and are the reason, along with the short incubation time, that the NPs are mainly located outside the cells. This was confirmed visually after washing the cells (data not shown). Delivery of UVC scintillating particles into cells rather than simply near them, is likely to yield greater enhancement of lethality upon exposure to X-rays, because UVC radiation is strongly absorbed by cytoplasm. This hypothesis remains to be tested.

To our knowledge there is no literature regarding the toxicity of $LuPO_4$. However, since $LuPO_4$ is a chemically stable compound, and insoluble in most solvents, toxicity is assumed to be low, similar to the toxicity of gold NPs. Literature describe only a minimal toxicity for gold NPs with particle sizes larger than 50 nm [6]. Our in *vitro* data suggest a concentration-dependent increase of nonspecific toxicity of the NPs tested (Fig. 5). This observation is reflected by the decrease in the surviving fraction to about 65 and 75% for the non-irradiated samples incubated with 5.0 and 7.5 mg × ml^{-1}, respectively. Lower concentrations (0.5, 1.0,

and 2.5 mg × ml^{-1}) $LuPO_4:Pr^{3+}$ did not show a significant decrease in viability and suggest a minimal toxicity on the cellular level. We confirmed no significant toxicity for the NPs at lower concentration using two different cell lines for longer time points up to 48 h (data not shown). No significant changes in toxicity were observed between 30 min and up to 48 h incubation. This result suggests no long term *in vitro* toxicity of the NPs for concentrations below 5.0 mg × ml. The unspecific toxicity of the NPs at higher concentrations might be due to mechanical interaction of the NPs with the surface of the cell membrane. Organ toxicity and concentration limits *in vivo* need to be tested in future animal experiments.

For a nanoparticle concentration of 0.5 mg × ml^{-1} a small and non-significant decrease in viability was observed compared to the cells irradiated with X-rays alone. With increasing NP concentration, the viability decreased and reached the highest effect for a $LuPO_4:Pr^{3+}$ concentration of 7.5 mg × ml^{-1}, while the unirradiated control showed moderate but significant unspecific toxicity of the NP. In contrast, 2.5 mg × ml^{-1} $LuPO_4:Pr^{3+}$ showed a significant cell killing effect when combined with radiation but no unspecific toxicity. Thus, our data suggest an optimal concentration of 2.5 mg × ml^{-1} $LuPO_4:Pr^{3+}$ for in *vitro* cell culture irradiation experiments. The observed effect appears to be synergistic, since the difference of the surviving fraction between radiation alone and combined treatment of about 20% is larger than the combined decrease of the unspecific NP toxicity and the irradiation alone. Based on our dose response curve as well as literature data for human fibroblasts [17,18], our combined treatment with 2.5 mg × ml^{-1} $LuPO_4:Pr^{3+}$ and 2 Gy X-ray is equal to a single X-ray dose of about 4 Gy.

The UV sensitive cell line XP17BE was used to evaluate the role of UV-induced DNA damage from particle emission during X-ray exposure. This cell line expresses a recessive autosomal genetic disorder of UV DNA damage repair [23,24]. Due to the reduced ability to repair UV damage these cells are 30–60% more sensitive to UV radiation compared to normal fibroblast cells [25–28]. As shown in Fig. 5, combined treatment reduced the surviving fraction of HFF1 to 25%, whereas XP17BE showed a higher reduction down to 15%. The surviving fraction measured for the XP17BE cells is about 40% lower compared to the treated HFF1 cells. This finding is in accordance with the reduced UV damage repair capacity of 30% that has been described in literature.

UV radiation causes specific DNA base damage in the form of pyrimidine photoproducts. Two of the major products are CPDs and 6-4PPs. In contrast to single and double strand breaks, it takes up to 24–48 h to completely repair these lesions [29]. Pyrimidine photoproducts usually occur in the ratio of 75% CPDs and 25% 6-4PPs [30]. The formation of CPDs was measured to confirm the presence of UV-induced DNA damage. The investigation of the induced CPDs after combined treatment reveals a significantly higher formation of CPDs compared to X-rays or $LuPO_4:Pr^{3+}$ alone. Our normalized data (Fig. 6b) suggest for a combined treatment with 2.5 mg × ml^{-1} $LuPO_4:Pr^{3+}$ and 4 Gy, that the generated amount of CPDs is similar to that from an UVC dose (254 nm) of about 15 J × m^{-2}.

The outcome of this work indicates an increased cell death using the combined treatment with X-rays and UV emitting $LuPO_4$: Pr^{3+} NPs. The investigation of the formation of CPDs

as UV specific DNA damage as well as the demonstrated increased sensitivity of XP17BE cells compared to HFF1 cells suggest a higher cell toxicity due to the involvement of locally generated UV photons. Our data also indicate a synergetic effect of the $LuPO_4:Pr^{3+}$ nanoparticles in combination with X-rays. Further, the loss of viability with the combined treatment using 2 Gy X-ray and 2.5 mg × ml^{-1} $LuPO_4$: Pr^{3+}, is equal to a treatment of about 4 Gy alone. Higher NP concentrations show a higher dose equivalent of up to 8 Gy, but also show an increase in unspecific toxicity of the $LuPO_4:Pr^{3+}$ NPs. Combining $LuPO_4:Pr^{3+}$ with ionizing radiation results in a local increase of the dose, which can be useful for increased tumor control or could allow lowering the radiation dose to spare the surrounding normal tissue with the same tumor control.

Further experiments are necessary to investigate the cytotoxicity of the generated UVC radiation under hypoxia to improve the treatment of hypoxic tumors. The NPs also need to be optimized in size, shape, and surface characteristics to minimize agglomeration, enhance stability, longevity, *in vivo* toxicity, and potential to add molecular tags specific for tumors. It is expected that optimizing the NPs and their delivery into cells will improve toxicity and tumor control, due to the shorter distance of the NPs to the DNA in the nucleus.

Acknowledgements

The authors are grateful to Radiation Monitoring Devices, Inc. for providing the $LuPO_4:Pr^{3+}$ NPs and Thomas Juestel from Munster University of Applied Sciences for the spectroscopic analysis. We also thank H. Frederick Dylla for fruitful discussions. This work was supported by the National Cancer Institute of the National Institutes of Health under award number 1R41CA206645-01A1.

References

[1]. Stewart BW, Wild CP, editors. World cancer report 2014. Lyon: International Agency for Research on Cancer; 2014.

[2]. Delaney G, Jacob S, Featherstone C, Barton M. The role of radiotherapy in cancer treatment estimating optimal utilization from a review of evidence-based clinical guidelines. Cancer 2005;104:1129–37. 10.1002/cncr.21324. [PubMed: 16080176]

[3]. Moeller BJ, Richardson RA, Dewhirst MW. Hypoxia and radiotherapy: Opportunities for improved outcomes in cancer treatment. Cancer Metastasis Rev 2007;26:241–8. 10.1007/s10555-007-9056-0· [PubMed: 17440683]

[4]. Rodemann HP, Bamberg M. Cellular basis of radiation-induced fibrosis. Radiother Oncol 1995;35:83–90. 10.1016/0167-8140(95)01540-W. [PubMed: 7569029]

[5]. Bentzen SM. Preventing or reducing late side effects of radiation therapy: radiobiology meets molecular pathology. Nat Rev Cancer 2006;6:702–13. 10.1038/nrc1950. [PubMed: 16929324]

[6]. Haume K, Rosa S, Grellet S, Smialek M, Butterworth K, Solov'yov A, Prise K, Golding J, Mason N. Gold nanoparticles for cancer radiotherapy: a review. Cancer Nano 2016;7 10.1186/s12645-016-0021-x.

[7]. Her S, Jaffray DA, Allen C. Gold nanoparticles for applications in cancer radiotherapy: mechanisms and recent advancements. Adv Drug Deliv Rev 2015;109:84–101. 10.1016/j.addr.2015.12.012. [PubMed: 26712711]

[8]. Maggiorella L, Barouch G, Devaux C, Pottier A, Deutsch E, Bourhis J, et al. Nanoscale radiotherapy with hafnium oxide nanoparticles. Futur Oncol 2012;8:1167–81. 10.2217/fon.12.96.

[9]. Song G, Liang C, Gong H, Li M, Zheng X, Cheng L, et al. Core-Shell MnSe@Bi_2Se_3 fabricated via a cation exchange method as novel nanotheranostics for multimodal imaging and synergistic thermoradiotherapy. Adv Mater 2015;27:6110–7. 10.1002/adma.201503006. [PubMed: 26331476]

[10]. Rybak-smith MJ, Townley HE. Encyclopedia of nanotechnology In: Bhushan B, editor. Encycl. Nanotechnol.. Dordrecht: Springer; 2015 p. 1–12. 10.1007/978-94-017-9780-1.

[11]. Cadet J, Sage E, Douki T. Ultraviolet radiation-mediated damage to cellular DNA. Mutat Res Fundam Mol Mech Mutagen 2005;571:3–17. 10.1016/j.mrfmmm.2004.09.012.

[12]. Srivastava AM, Jennings M, Collins J. The interconfigurational ($4f^15d^1 \rightarrow 4f^2$) luminescence of Pr^{3+} in $LuPO_4$, $K_3Lu(PO_4)_2$ and $LiLuSiO_4$. Opt Mater (Amst) 2012;34:1347–52. 10.1016/j.optmat.2012.02.016·

[13]. Milligan WO, Mullica DF, Beall GW, Boatner LA. Structural investigations of YPO_4, $ScPO_4$, and LuPO4. Inorg Chim Acta 1982;60:39–43. 10.1016/S0020-1693(00)91148-4.

[14]. Squillante MR, Jüstel T, Anderson RR, Brecher C, Chartier D, Christian JF, Cicchetti N, Espinoza S, McAdams DR, Muller M, Tornifoglio B, Wang Y, Purschke M. Fabrication and characterization of UV-emitting nanoparticles as novel radiation sensitizers targeting hypoxic tumor cells. Opt Mater 2018;80:197–202. 10.1016/j.optmat.2018.04.033.

[15]. Anderson RR, Parrish JA. The optics of human skin. J Invest Dermatol 1981;77:13–9. 10.1016/j.artres.2008.11.002. [PubMed: 7252245]

[16]. Stylianopoulos T, Jain RK. Design considerations for nanotherapeutics in oncology. Nanomedicine Nanotechnol Biol Med 2015;11:1893–907. 10.1016/j.nano.2015.07.015.

[17]. Li HK, Matsumoto Y, Furusawa Y, Kamada T. PU-H71, a novel Hsp90 inhibitor, as a potential cancer-specific sensitizer to carbon-ion beam therapy. J Radiat Res 2016;57:572–5. 10.1093/jrr/rrw054. [PubMed: 27242340]

[18]. Suzuki K, Kodama S, Watanabe M, Cells D. Extremely low-dose ionizing radiation causes activation of mitogen-activated protein kinase pathway and enhances proliferation of normal human diploid cells extremely low-dose ionizing radiation causes activation of mitogen-activated protein kinase Pathwa. Cancer Res 2001;61:5396–401. Published July. [PubMed: 11454682]

[19]. Retif P, Pinel S, Toussaint M, Frochot C, Chouikrat R, Bastogne T, et al. Nanoparticles for radiation therapy enhancement: The key parameters. Theranostics 2015;5:1030–44. 10.7150/thno.11642. [PubMed: 26155318]

[20]. Kielbassa C, Roza L, Epe B. Wavelength dependence of oxidative DNA damage induced by UV and visible light. Carcinogenesis 1997;18:811–6. 10.1093/carcin/18.4.811. [PubMed: 9111219]

[21]. Taylor CR, Anderson RR, Gange RW, Michaud NA, Flotte TJ. Light and electron microscopic analysis of tattoos treated by Q-switched ruby laser. J Invest Dermatol 1991;97:131–6. 10.1111/1523-1747.ep12478570. [PubMed: 2056183]

[22]. Jain S, Coulter JA, Butterworth KT, Hounsell AR, Mcmahon SJ, Hyland WB, et al. Gold nanoparticle cellular uptake, toxicity and radiosensitisation in hypoxic conditions. Radiother Oncol 2014;110:342–7. 10.1016/j.radonc.2013.12.013. [PubMed: 24444528]

[23]. Kraemer KH, Lee MM, Scotto J. Xeroderma pigmentosum: cutaneous, ocular, and neurologic abnormalities in 830 published cases. Arch Dermatol 1987;123:241–50. 10.1001/archderm.1987.01660260111026. [PubMed: 3545087]

[24]. De Gruijl FR, Van Kranen HJ, Mullenders LHF. UV-induced DNA damage, repair, mutations and oncogenic pathways in skin cancer. J Photochem Photobiol B Biol 2001;63:19–27. 10.1016/S1011-1344(01)00199-3.

[25]. Cleaver JE, Thomas GH. Rapid diagnosis of sensitivity to ultraviolet light in fibroblasts from dermatologic disorders, with particular reference to xeroderma pigmentosum. J Invest Dermatol 1988;90:467–71. 10.1111/1523-1747.ep12460917. [PubMed: 3351331]

[26]. Mccormick JJ, Kateley-kohler S, Watanabe M, Ma VM. Abnormal sensitivity of human fibroblasts from xeroderma pigmentosum variants to transformation to anchorage independence by ultraviolet radiation. Cancer Res. 1986;46:489–92. Published February. [PubMed: 3940626]

[27]. Cleaver JE. DNA repair and radiation sensitivity in human (xeroderma pigmentosum) cells. Int J Radiat Biol 1970;18:557–65. 10.1080/09553007014551491.

[28]. Boyle J, Ueda T, Oh KS, Imoto K, Tamura D, Jagdeo J, et al. Persistence of repair proteins at unrepaired DNA damage distinguishes diseases with ERCC2 (XPD) mutations: Cancer-prone xeroderma pigmentosum vs. non-cancer-prone trichothiodystrophy. Hum Mutat 2008;29:1194–208. 10.1002/humu.20768. [PubMed: 18470933]

[29]. Nakagawa A, Kobayashi N, Muramatsu T, Yamashina Y, Shirai T, Hashimoto MW, et al. Three-dimensional visualization of ultraviolet-induced DNA damage and its repair in human cell nuclei. J Invest Dermatol 1998;110:143–8. 10.1046/j.1523-1747.1998.00100.x. [PubMed: 9457909]

[30]. Sinha RP, Häder D-P. UV-induced DNA damage and repair: a review. Photochem Photobiol Sci 2002;1:225–36. 10.1039/b201230h. [PubMed: 12661961]

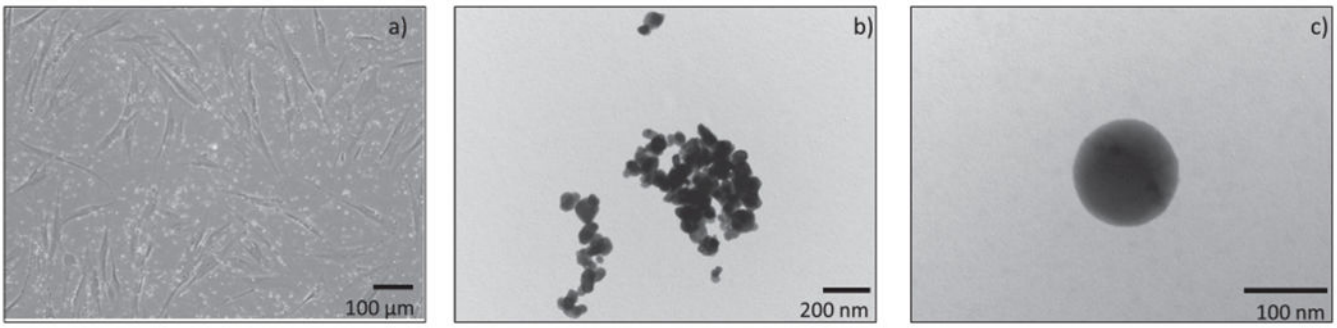

Fig. 1.

Inverted microscope image of the $LuPO_4:Pr^{3+}$ NPs in HFF1 cell culture at 100× magnification (a) (contrast and saturation was adjusted for clarification). The “bright dots” in the picture are the NPs. TEM image of the $LuPO_4:Pr^{3+}$ NPs at magnification of 15500× (b) and 52000× (c). The NPs show a smooth surface and a spherical shape. Some agglomerations were detected.

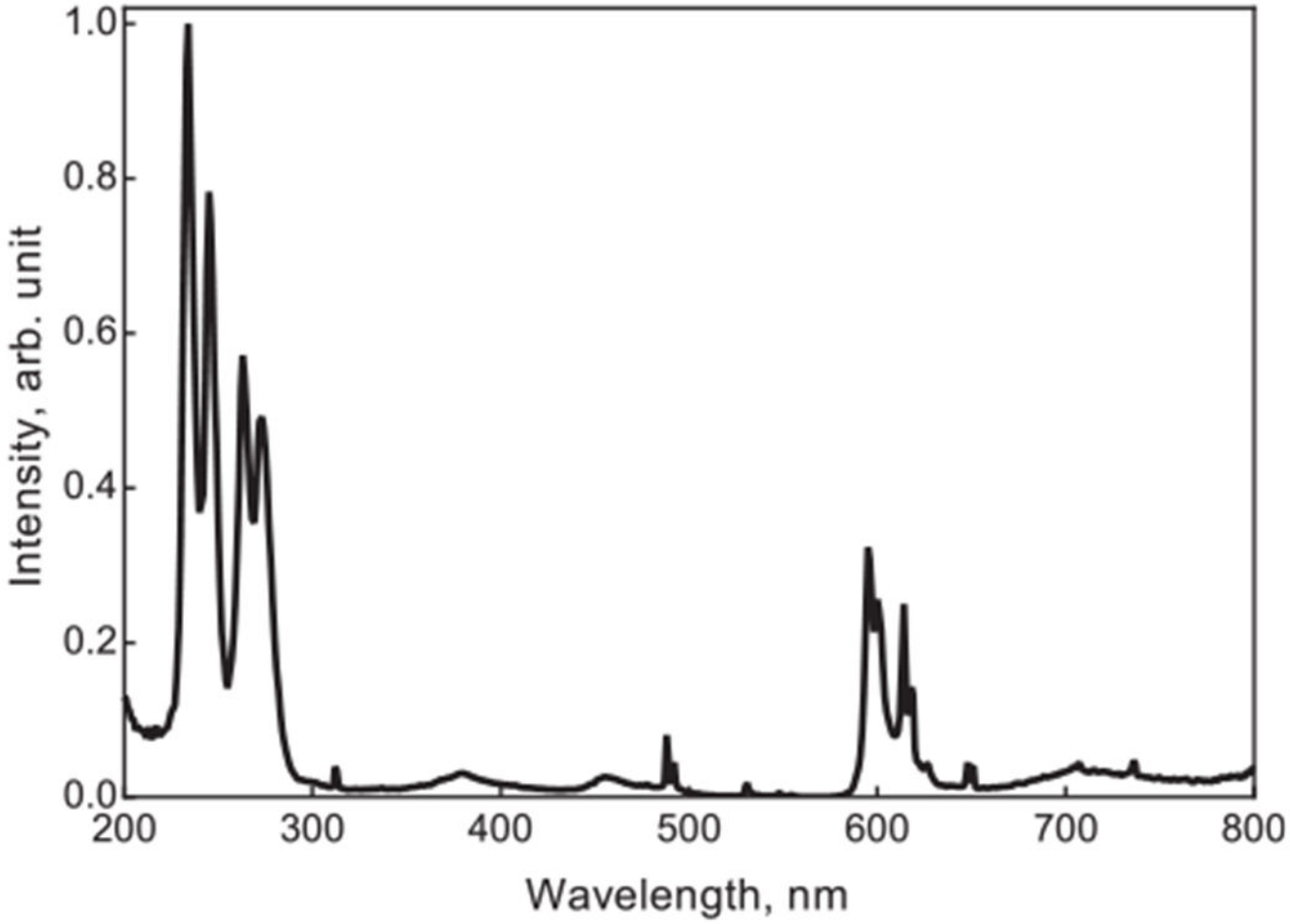

Fig. 2.

Emission spectrum of $LuPO_4:Pr^{3+}$ after X-ray excitation. The emission between 220 and 285 nm is due to the inter-configurational $4f^1 5d^1$-$4f^2$ transition in Pr^{3+}. The emission above 300 nm is attributed to the to the intra-configurational $4f^2$-$4f^2$ transition in Pr^{3+}.

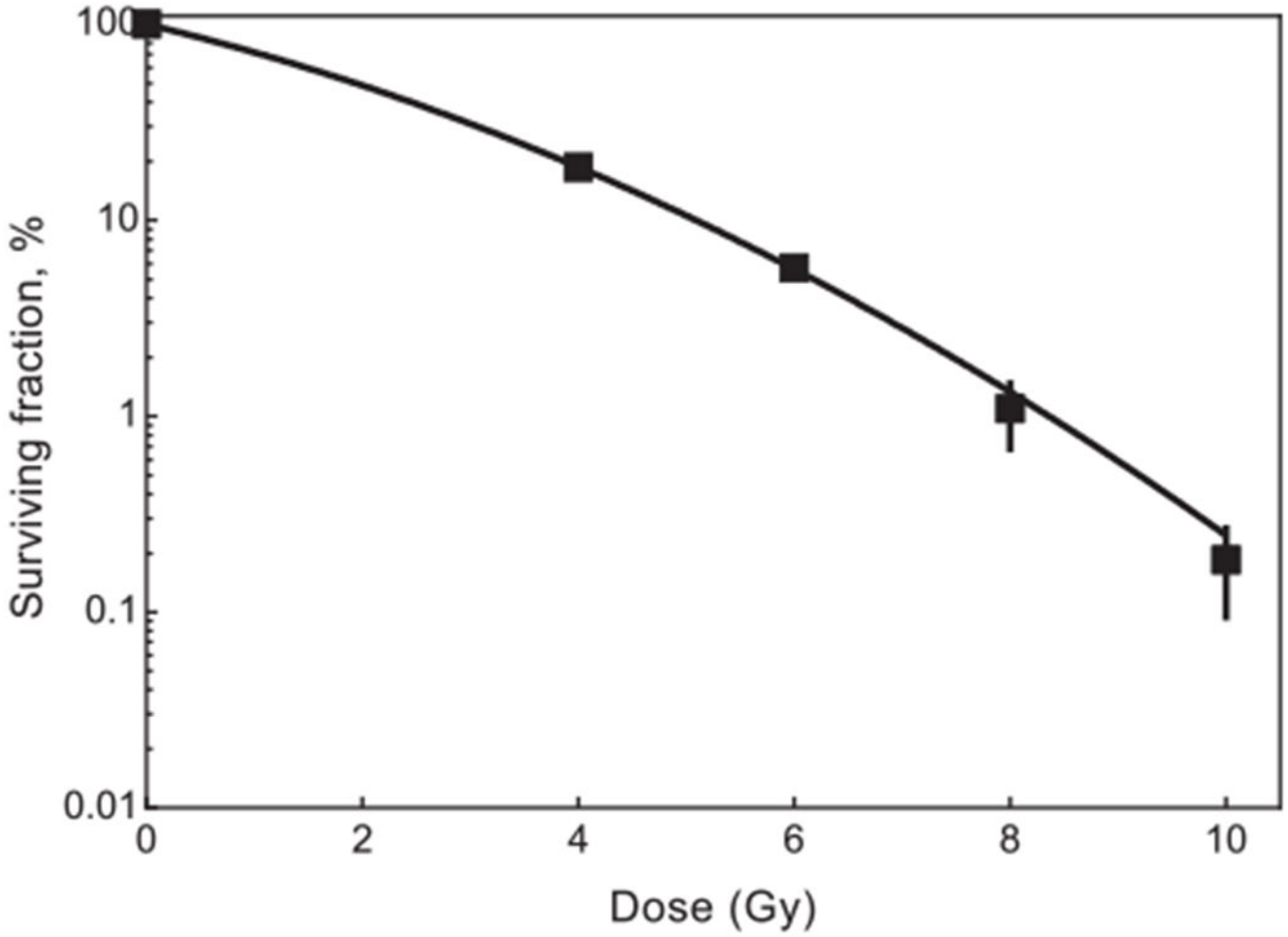

Fig. 3.

Dose response curve for HFF1 after irradiation with X-ray up to 10 Gy. Error bars represent the standard error of mean and each data point represents at least $_4$ independent experiments.

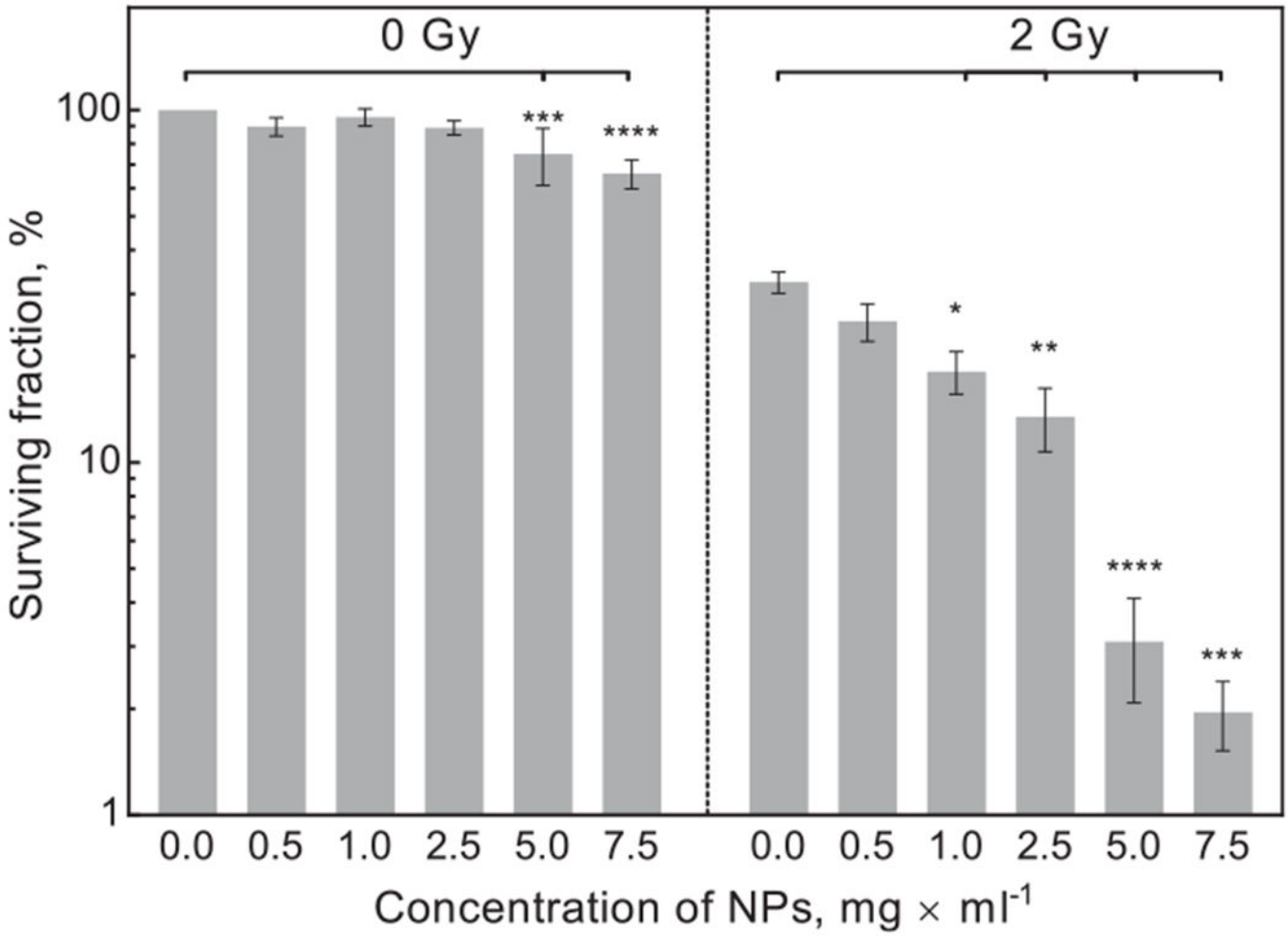

Fig. 4.

Clonogenic survival of HFF1 cells treated with different concentrations of $LuPO_4:Pr^{3+}$. Right side of the graph shows the surviving fraction before irradiation and left side after irradiation with 2 Gy. Error bars represent standard error of mean, each bar represents at least 8 independent experiments.

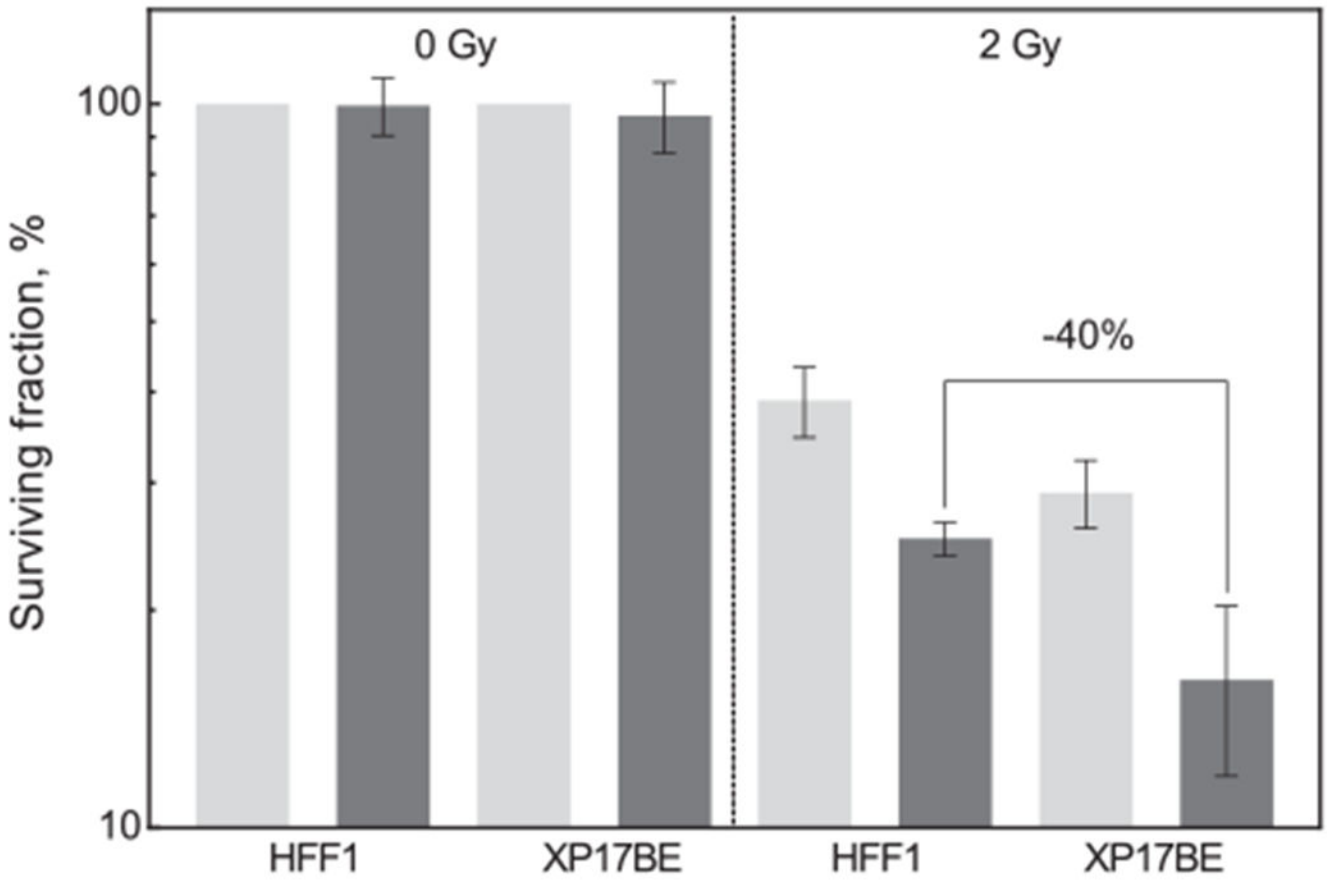

Fig. 5.

Surviving fraction of HFF1 and XP17BE cells after a combined treatment with 2 Gy and 2.5 mg × ml^{-1} $LuPO_4$:Pr^{3+} NPs. Right side of the graph shows the surviving fraction before irradiation and left side irradiation. The surviving fraction of the XP17BE cells is approximately 40% lower than for the treated HFF1 cells. Light gray: without NPs, dark gray: with NPs. Error bars represent standard error of mean, and each bar represents at least 3 independent experiments.

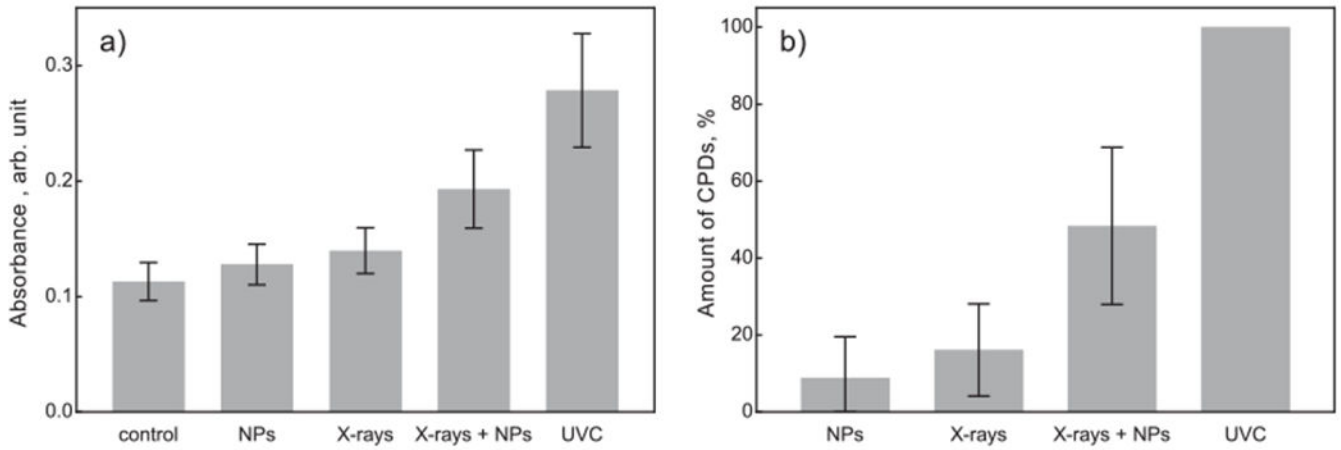

Fig. 6.

Detection of CPDs for HFF1 cells after combined treatment with 4 Gy and 2.5 mg × ml^{-1} $LuPO_4:Pr^{3+}$ NPs. Absorbance at 450 nm (a) and amount of CPDs (b). In (b) data are normalized to a UV dose of 60 J × m^{-2} at 254 nm and the untreated control (100% and 0% respectively). Error bars represent standard error of mean, and each bar represents at least 7 independent experiments.